Elliptic Flow and Nuclear Modification Factor in Ultrarelativistic Heavy-Ion Collisions within a Partonic Transport Model

Jan Uphoff,[1,*] Florian Senzel,[1] Oliver Fochler,[1] Christian Wesp,[1] Zhe Xu,[2] and Carsten Greiner[1]
[1]Institut für Theoretische Physik, Goethe-Universität Frankfurt, Max-von-Laue-Strasse 1, D-60438 Frankfurt am Main, Germany
[2]Department of Physics, Tsinghua University, Beijing 100084, China

(Received 11 February 2014; revised manuscript received 17 February 2015; published 17 March 2015)

The quark gluon plasma produced in ultrarelativistic heavy-ion collisions exhibits remarkable features. It behaves like a nearly perfect liquid with a small shear viscosity to entropy density ratio and leads to the quenching of highly energetic particles. We show that both effects can be understood for the first time within one common framework. Employing the parton cascade Boltzmann approach to multiparton scatterings, the microscopic interactions and the space-time evolution of the quark gluon plasma are calculated by solving the relativistic Boltzmann equation. Based on cross sections obtained from perturbative QCD with explicitly taking the running coupling into account, we calculate the nuclear modification factor and elliptic flow in ultrarelativistic heavy-ion collisions. With only one single parameter associated with coherence effects of medium-induced gluon radiation, the experimental data of both observables can be understood on a microscopic level. Furthermore, we show that perturbative QCD interactions with a running coupling lead to a sufficiently small shear viscosity to entropy density ratio of the quark gluon plasma, which provides a microscopic explanation for the observations stated by hydrodynamic calculations.

DOI: 10.1103/PhysRevLett.114.112301 PACS numbers: 24.85.+p, 12.38.Mh, 24.10.Lx, 25.75.-q

In ultrarelativistic heavy-ion collisions at the Relativistic Heavy-Ion Collider (RHIC) at BNL and the Large Hadron Collider (LHC) at CERN, a hot and dense medium is created that consists of quarks and gluons. Experimental data show that this quark gluon plasma (QGP) possesses a strong collective behavior and that high-energy partons deposit a sizable amount of their energy in this medium [1,2].

The collective behavior is often quantified by the elliptic flow coefficient v_2, which is the second harmonic of the Fourier decomposition of the azimuthal angle distribution of particle yields. Comparisons to hydrodynamic calculations reveal that the QGP behaves like a nearly perfect liquid with a small shear viscosity to entropy density ratio [3,4]. However, the microscopic reason for this small ratio is currently not understood.

Experimental data of the nuclear modification factor R_{AA}, which is defined as the yield in heavy-ion $(A+A)$ collisions divided by the yield in proton-proton $(p+p)$ collisions scaled with the number of binary collisions:

$$R_{AA} = \frac{d^2N_{AA}/dp_T dy}{N_{\mathrm{bin}} d^2N_{pp}/dp_T dy} \tag{1}$$

and the momentum imbalance of fully reconstructed jets indicate that high-energy particles are quenched by the created medium and lose lots of their energy [1,2]. Several calculations based on perturbative QCD (pQCD) energy loss in the QGP can describe the experimental data [5–12].

A simultaneous understanding of collective bulk phenomena and jet quenching on the microscopic level remains a challenge, although several partonic transport models [13–19] have been developed to address this issue. In this Letter, we will present new results on both observables obtained with the partonic transport model *Boltzmann approach to multiparton scatterings* (BAMPS). Based on cross sections calculated in pQCD, soft and hard particles are treated on the same footing in a common framework. While we take explicitly the running of the coupling into account, we study not only the energy loss of highly energetic particles but also the collective behavior of the bulk medium.

After a short introduction to BAMPS and the underlying physics, we address the employed pQCD cross sections and how the Landau-Pomeranchuk-Migdal (LPM) effect is implemented in our approach. Subsequently, we compare our results for R_{AA} and v_2 with experimental data at RHIC and LHC and study the averaged value of the running coupling and the shear viscosity to entropy density ratio of the QGP for deeper insights into the properties of the hot and dense matter.

The partonic transport model BAMPS [17,20] describes the $3+1$ dimensional evolution of the QGP phase by solving the Boltzmann equation for on-shell partons. All $2 \to 2$ *and* $2 \leftrightarrow 3$ processes for light quarks (number of flavors $n_f = 3$, $q = u, d, s$) and gluons (g) are included employing pQCD cross sections. In contrast to earlier BAMPS calculations, the coupling α_s is not assumed to be fixed, but its running is explicitly taken into account by setting the scale to the momentum transfer of the considered channel. This is done analogously to the

implementation of heavy quarks in BAMPS [21,22]. For the effective parameterization of the running coupling, the one-loop coupling has been continued to the timelike region according to Ref. [23]; see also Ref. [24] for details. The maximum value of the coupling in the soft region can be constrained by universality arguments to be around $\alpha_{s;\max} = 1.0$ [25,26]. Since we tested that varying the maximum value between 0.8 and 2 does not affect either the transport cross section or energy loss of soft as well as hard particles in a static medium or the integrated flow v_2 of an expanding heavy-ion medium, we set the maximum value to $\alpha_{s;\max} = 1.0$ and do not expect a sensitivity of the following results on this value.

The initial parton distributions are obtained from PYTHIA [27] and the Monte Carlo Glauber model as described in detail in Refs. [17,28]. Since the initial condition in one BAMPS run is a collection of N_{test} individual real events, potential initial event-by-event fluctuations are washed out by $1/N_{\text{test}}$ [17].

In Ref. [29], we have recently presented an improved version of the Gunion-Bertsch (GB) matrix element for $2 \leftrightarrow 3$ processes, which cures problems of the original matrix element [30] at forward and backward rapidity of the emitted gluon. Numerical comparisons to the exact matrix element show good agreement [29].

Within the GB approximation, the improved GB matrix element for the process $X \to Y + g$ factorizes in the binary matrix element for $X \to Y$ and a radiative factor P_g [29]:

$$|\overline{\mathcal{M}}_{X\to Y+g}|^2 = |\overline{\mathcal{M}}_{X\to Y}|^2 P_g \tag{2}$$

with

$$P_g = 48\pi\alpha_s(k_\perp^2)(1-\bar{x})^2 \times \left[\frac{\mathbf{k}_\perp}{k_\perp^2} + \frac{\mathbf{q}_\perp - \mathbf{k}_\perp}{(\mathbf{q}_\perp - \mathbf{k}_\perp)^2 + m_D^2[\alpha_s(k_\perp^2)]}\right]^2. \tag{3}$$

The transverse momentum of the emitted and internal gluons is denoted with $\mathbf{k}_\perp$ and $\mathbf{q}_\perp$, respectively. The longitudinal momentum fraction $\bar{x}$ is related to the rapidity of the emitted gluon via $\bar{x} = k_\perp e^{|y|}/\sqrt{s}$, where s is the squared center of mass energy of the interaction. $X \to Y$ stand for any binary process of light quarks and gluons, while only (Mandelstam) t channel dominated processes (equivalent to $X = Y$) have a finite contribution within the GB approximation. These binary matrix elements are given in the same approximation by

$$|\overline{\mathcal{M}}_{X\to Y}|^2 = C_{X\to Y} 64\pi^2\alpha_s^2(t)\frac{s^2}{\{t - m_D^2[\alpha_s(t)]\}^2}, \tag{4}$$

where $C_{X\to Y}$ is the color factor of the respective process. All internal gluon propagators in Eqs. (3) and (4) are screened with the Debye mass m_D. The coupling in the definition of the Debye mass is also evaluated at the respective scale of the propagators. The first term in the brackets in Eq. (3) does not need to be screened by a screening mass, since it corresponds to the external emitted gluon and the infrared divergence is cured by the implementation of the LPM effect in BAMPS [17]. Since including coherence effects consistently in a semiclassical transport model is difficult, the LPM suppression is effectively implemented by only allowing completely independent scatterings, demanding that the formation time τ of the emitted gluon is smaller than the mean free path λ of the emitting particle. To this end, the LPM effect is included in BAMPS via a Θ function in the integrand of the $2 \leftrightarrow 3$ cross section [17]:

$$\Theta(\lambda - X_{\text{LPM}}\tau). \tag{5}$$

$X_{\text{LPM}} = 0$ corresponds to no LPM suppression, while $X_{\text{LPM}} = 1$, the previously [17] used value in BAMPS, discards all interfering processes altogether. We expect that a more sophisticated treatment of the LPM effect would allow also some interference processes, leading effectively to $0 < X_{\text{LPM}} < 1$. Thus, we treat X_{LPM} as a parameter and calibrate its value to the nuclear modification factor of neutral pions at RHIC. Studies within a static medium show that the energy loss of partons exhibits a nearly logarithmic dependence on the parameter X_{LPM}.

In the following, we present an update of previous calculations for the elliptic flow [31–34] and the nuclear modification factor [34–36], now including the improved GB cross section as well as a running coupling for all channels.

Figure 1 depicts the nuclear modification factor of light partons and neutral pions at RHIC. Because of the larger color factor, gluons are considerably more strongly suppressed than light quarks. For comparing with experimental

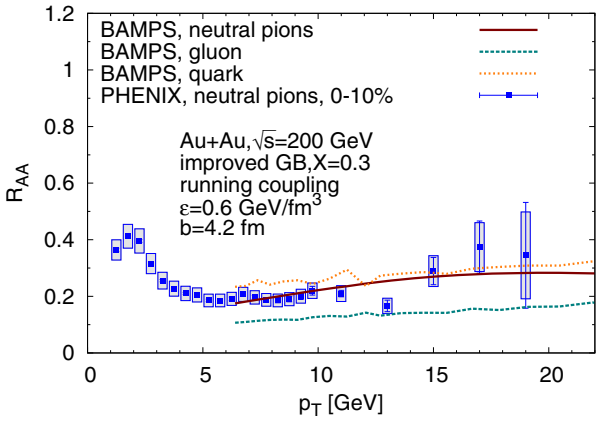

FIG. 1 (color online). Nuclear modification factor R_{AA} of gluons, light quarks, and neutral pions at RHIC for a running coupling and LPM parameter $X_{\text{LPM}} = 0.3$ together with data of neutral pions [39].

data of neutral pions, we perform the fragmentation of gluons and light quarks to neutral pions with the Albino-Kniehl-Kramer (AKK) fragmentation functions [37]. Studies with Kniehl-Kramer-Potter fragmentation functions [38] show that the particular choice of fragmentation functions does not affect the nuclear modification factor. The pion curve lies between the gluon and light quark curve. At small p_T the pions are dominated by fragmentation from gluons, and at large p_T from light quarks. The LPM parameter X_{LPM} is chosen as $X_{\mathrm{LPM}} = 0.3$ to give the best agreement with the data. In the following, we keep this parameter fixed and compare to other experimental data of the R_{AA} and v_2 at RHIC and LHC. As we explained above, an X_{LPM} smaller than one should be consistent with a more sophisticated LPM treatment in BAMPS.

With $X_{\mathrm{LPM}} = 0.3$ we find very good agreement with the experimental data at RHIC. The same holds at LHC, as is shown in Fig. 2. In addition to the gluon and light quark curves, we also depict the curve for charged hadrons obtained again via AKK fragmentation. Again, the hadron curve lies mainly between the light quark and gluon curves but is slightly larger than the light quark curve for large p_T. Because of the fragmentation process, a hadron possesses on average a transverse momentum of only about half of its parental light parton; that is, the charged hadron R_{AA} at a given p_T has approximately the same value as the parton R_{AA} at twice as large p_T. Because of the rise in the R_{AA}, the hadron curve is shifted to larger values than the parton curve at the same p_T. Furthermore, the slope of the hadron curve at intermediate p_T is steeper than the parton curves due to the fragmentation process as well as the different slopes of the gluon and light quark spectra. Hadrons at large p_T are dominated by quark fragmentation, while hadrons at small p_T are dominated by gluon fragmentation.

Having presented the results for high-energy particles, we now address the bulk medium interactions. It is important to note that all partons in BAMPS are treated on the same footing; that is, all particles interact based on the pQCD cross sections introduced above. Since hadronization from the partonic to the hadronic phase is not well understood in the soft regime, we compare the *integrated* v_2 on the parton level to experimental data, as the integrated v_2 should not be sensitive to the phase transition.

In Figs. 3 and 4, the integrated elliptic flow is shown as a function of the number of participants at RHIC and LHC, respectively. With the same parameter $X_{\mathrm{LPM}} = 0.3$ we obtain a sizable elliptic flow on the parton level, which is calculated after a partonic freeze-out energy density of $\epsilon = 0.6\ \mathrm{GeV/fm^3}$ is reached [32]. The gluon elliptic flow is close to the data and the light quark v_2 smaller due to the smaller color factor. The integrated v_2 of all light partons is the curve that should be compared to the data. It is slightly smaller than the data, since hadronic final interactions and event-by-event fluctuations in the initial state are not taken into account. As shown in Ref. [41], hadronic contributions may increase the v_2 by about 10%–15%, which could explain part of the small deviation between the light parton curve and the experimental data. Furthermore, explicit consideration of quantum statistics could increase the elliptic flow due to Bose enhancement of gluons, while the nuclear modification factor of high-energy particles is not influenced. We also studied the sensitivity of the elliptic flow and nuclear modification factor on the LPM parameter X_{LPM} and found that the elliptic flow is less sensitive than the nuclear modification factor. Thus the conclusion of a sizable elliptic flow is a solid statement. However, for more quantitative studies—in particular, for high-p_T v_2—a more sophisticated treatment of the LPM effect is necessary, which is planned for the future.

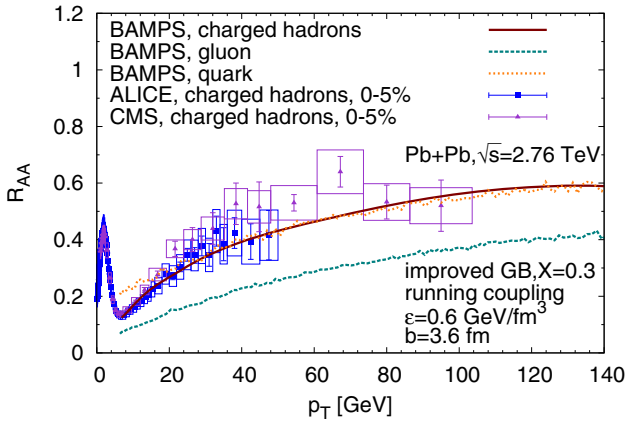

FIG. 2 (color online). Nuclear modification factor R_{AA} of gluons, light quarks, and charged hadrons at LHC for a running coupling and LPM parameter $X_{\mathrm{LPM}} = 0.3$ together with data of charged hadrons [40].

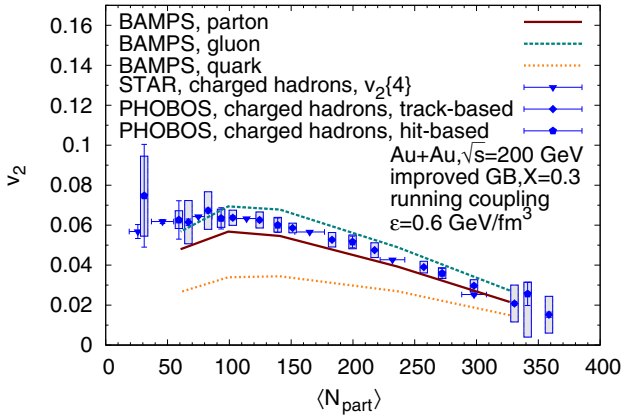

FIG. 3 (color online). Elliptic flow v_2 of gluons, light quarks, and both together (light partons) within $|\eta| < 1.0$ as a function of the number of participants N_{part} at RHIC for a running coupling and LPM parameter $X_{\mathrm{LPM}} = 0.3$. As a comparison, we show experimental data by STAR and PHOBOS for charged hadrons within $|\eta| < 0.5$ and $|\eta| < 1.0$ [42,43].

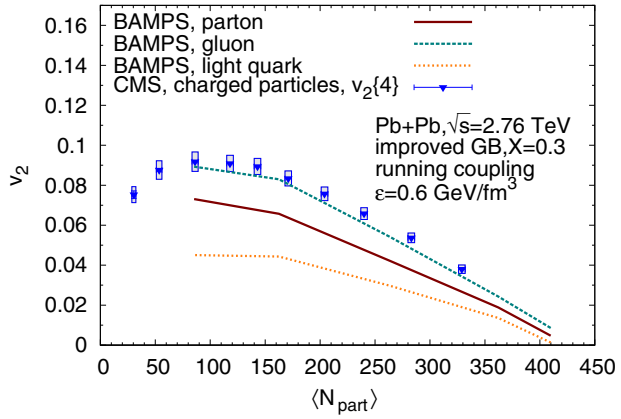

FIG. 4 (color online). Elliptic flow v_2 of gluons, light quarks, and both together (light partons) within $|\eta| < 0.8$ as a function of the number of participants N_{part} at LHC for a running coupling and LPM parameter $X_{\mathrm{LPM}} = 0.3$. As a comparison, we show experimental data by CMS for charged hadrons within $|\eta| < 0.8$ [44].

It is a remarkable result that we obtain a sizable v_2 while having the same suppression as the experimental data at large p_T. The reason for this lies partly in the isotropization of inelastic $2 \leftrightarrow 3$ processes and partly in the running coupling. For particles with small p_T, the coupling is on average stronger than for high-energy particles, which affects the elliptic flow at small p_T and R_{AA} at large p_T differently. In Fig. 5, the averaged running coupling of binary collisional processes is depicted in a static thermal medium as a function of the temperature of the medium, where the coupling is evaluated microscopically at the momentum transfer of each interaction. As expected, the average coupling decreases with increasing temperature. These averages result from a broad distribution: While small couplings lead to the observed jet quenching and flow, large couplings, which are potentially problematic for the applicability of pQCD, have a nearly negligible effect for R_{AA} and v_2 due to their small momentum transfers. Consequently, the seemingly large average values of the coupling shown in Fig. 5 do not accurately reflect the physical influence of the running coupling. Since we evaluate the coupling at the corresponding momentum transfer of each process, it is obviously not true that all processes have this large mean coupling: Physically relevant processes with a large transport cross section have a much smaller coupling, while physically unimportant processes with a small transport cross section have couplings close to the cutoff.

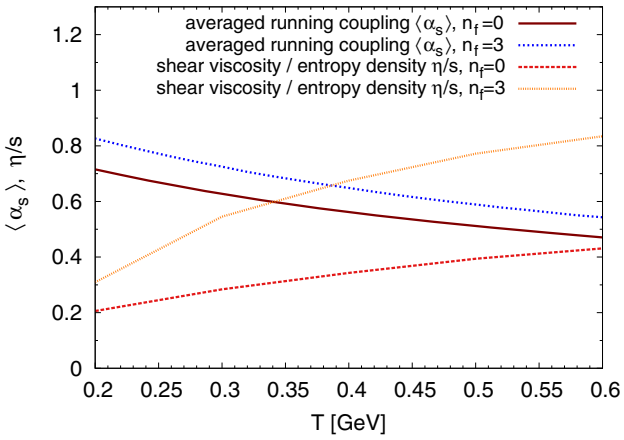

FIG. 5 (color online). Shear viscosity over entropy density η/s for running coupling and $X_{\mathrm{LPM}} = 0.3$ in a static medium of temperature T with number of quark flavors n_f. Furthermore, the average value of the running coupling for binary collisions in a thermal medium of temperature T is shown.

As advocated in dissipative hydrodynamic fits, an important quantity for the bulk medium in heavy-ion collisions is the shear viscosity to entropy density ratio η/s. In Fig. 5, the temperature dependence of this value in a static medium allowing all $2 \to 2$ and $2 \leftrightarrow 3$ is shown. The shear viscosity is calculated via the Green-Kubo relation, which links the autocorrelation function of the medium energy-momentum tensor of the medium to the transport coefficient η [45]. The ratio η/s decreases with decreasing temperature and reaches a minimum at the phase transition. The region that is most relevant for the elliptic flow lies around $T = 0.2$ GeV for $n_f = 0$ (the QGP at RHIC and LHC is mostly gluon dominated; in our calculation, the gluon and quark fugacity at freeze-out at LHC take values of approximately 0.9 and 0.5, respectively). Here, the value of η/s is approximately 0.2, which agrees very well with the shear viscosity extraction from dissipative hydrodynamic models [46]. Thus, our calculation employing pQCD cross sections can give a microscopic explanation of the small shear viscosity to entropy density ratio extracted from hydrodynamics. As a note, even for small η/s in this region, Boltzmann transport with quasiparticles is still valid, because the quantal corrections of Kadanoff-Baym–type transport equations do not have dominant contributions [47,48].

In summary, we compared results on the nuclear modification factor and elliptic flow in ultrarelativistic heavy-ion collisions obtained from full microscopic, nonequilibrium transport calculations to experimental data. With pQCD cross sections and a running coupling, the experimental data can be understood on the parton level, although some contribution to the elliptic flow from hadronic interactions might be relevant. We show that these interactions lead to a sufficiently small shear viscosity to entropy density ratio and thus can provide a microscopic explanation of the small value extracted from viscous hydrodynamics. As a future project, it would be interesting to study possible improvements on the LPM effect [49,50] and include quantum statistics instead of Boltzmann statistics. Moreover, we will further investigate the energy loss of fully reconstructed jets [51] and heavy flavor [52,53] within the same framework.

This work was supported by the Bundesministerium für Bildung und Forschung (BMBF), the NSFC under Grant No. 11275103, HGS-HIRe, and the Helmholtz International Center for FAIR within the framework of the LOEWE program launched by the State of Hesse. Numerical computations have been performed at the Center for Scientific Computing (CSC).

*uphoff@th.physik.uni-frankfurt.de

[1] B. V. Jacak and B. Müller, Science **337**, 310 (2012).
[2] B. Müller, J. Schukraft, and B. Wyslouch, Annu. Rev. Nucl. Part. Sci. **62**, 361 (2012).
[3] C. Shen, U. Heinz, P. Huovinen, and H. Song, Phys. Rev. C **84**, 044903 (2011).
[4] C. Gale, S. Jeon, and B. Schenke, Int. J. Mod. Phys. A **28**, 1340011 (2013).
[5] A. Dainese, C. Loizides, and G. Paic, Eur. Phys. J. C **38**, 461 (2005).
[6] I. Vitev and M. Gyulassy, Phys. Rev. Lett. **89**, 252301 (2002).
[7] I. Vitev, J. Phys. G **30**, S791 (2004).
[8] C. A. Salgado and U. A. Wiedemann, Phys. Rev. D **68**, 014008 (2003).
[9] N. Armesto, A. Dainese, C. A. Salgado, and U. A. Wiedemann, Phys. Rev. D **71**, 054027 (2005).
[10] S. Wicks, W. Horowitz, M. Djordjevic, and M. Gyulassy, Nucl. Phys. **A784**, 426 (2007).
[11] B. Schenke, C. Gale, and S. Jeon, Phys. Rev. C **80**, 054913 (2009).
[12] T. Renk, H. Holopainen, R. Paatelainen, and K. J. Eskola, Phys. Rev. C **84**, 014906 (2011).
[13] K. Geiger and B. Müller, Nucl. Phys. **B369**, 600 (1992).
[14] B. Zhang, Comput. Phys. Commun. **109**, 193 (1998).
[15] D. Molnar and M. Gyulassy, Phys. Rev. C **62**, 054907 (2000).
[16] S. Bass, B. Müller, and D. Srivastava, Phys. Lett. B **551**, 277 (2003).
[17] Z. Xu and C. Greiner, Phys. Rev. C **71**, 064901 (2005).
[18] Z.-W. Lin, C. M. Ko, B.-A. Li, B. Zhang, and S. Pal, Phys. Rev. C **72**, 064901 (2005).
[19] M. Ruggieri, F. Scardina, S. Plumari, and V. Greco, Phys. Lett. B **727**, 177 (2013).
[20] Z. Xu and C. Greiner, Phys. Rev. C **76**, 024911 (2007).
[21] J. Uphoff, O. Fochler, Z. Xu, and C. Greiner, Phys. Rev. C **84**, 024908 (2011).
[22] J. Uphoff, O. Fochler, Z. Xu, and C. Greiner, Phys. Lett. B **717**, 430 (2012).
[23] Y. L. Dokshitzer, G. Marchesini, and B. R. Webber, Nucl. Phys. **B469**, 93 (1996).
[24] P. B. Gossiaux and J. Aichelin, Phys. Rev. C **78**, 014904 (2008).
[25] A. Peshier, Nucl. Phys. **A888**, 7 (2012).
[26] Y. Dokshitzer, Nucl. Phys. **A711**, 11 (2002).
[27] T. Sjostrand, S. Mrenna, and P. Skands, J. High Energy Phys. 05 (2006) 026.
[28] J. Uphoff, O. Fochler, Z. Xu, and C. Greiner, Phys. Rev. C **82**, 044906 (2010).
[29] O. Fochler, J. Uphoff, Z. Xu, and C. Greiner, Phys. Rev. D **88**, 014018 (2013).
[30] J. Gunion and G. Bertsch, Phys. Rev. D **25**, 746 (1982).
[31] Z. Xu, C. Greiner, and H. Stöcker, Phys. Rev. Lett. **101**, 082302 (2008).
[32] Z. Xu and C. Greiner, Phys. Rev. C **79**, 014904 (2009).
[33] Z. Xu and C. Greiner, Phys. Rev. C **81**, 054901 (2010).
[34] O. Fochler, J. Uphoff, Z. Xu, and C. Greiner, J. Phys. G **38**, 124152 (2011).
[35] O. Fochler, Z. Xu, and C. Greiner, Phys. Rev. Lett. **102**, 202301 (2009).
[36] O. Fochler, Z. Xu, and C. Greiner, Phys. Rev. C **82**, 024907 (2010).
[37] S. Albino, B. Kniehl, and G. Kramer, Nucl. Phys. **B803**, 42 (2008).
[38] B. A. Kniehl, G. Kramer, and B. Potter, Nucl. Phys. **B582**, 514 (2000).
[39] A. Adare *et al.* (PHENIX Collaboration), Phys. Rev. Lett. **101**, 232301 (2008).
[40] B. Abelev *et al.* (ALICE Collaboration), Phys. Lett. B **720**, 52 (2013).
[41] J. Auvinen and H. Petersen, Phys. Rev. C **88**, 064908 (2013).
[42] J. Adams *et al.* (STAR Collaboration), Phys. Rev. C **72**, 014904 (2005).
[43] B. Back *et al.* (PHOBOS Collaboration), Phys. Rev. C **72**, 051901 (2005).
[44] S. Chatrchyan *et al.* (CMS Collaboration), Phys. Rev. C **87**, 014902 (2013).
[45] C. Wesp, A. El, F. Reining, Z. Xu, I. Bouras, and C. Greiner, Phys. Rev. C **84**, 054911 (2011).
[46] C. Gale, S. Jeon, B. Schenke, P. Tribedy, and R. Venugopalan, Phys. Rev. Lett. **110**, 012302 (2013).
[47] Z. Xu and C. Greiner, Phys. Rev. Lett. **100**, 172301 (2008).
[48] S. Juchem, W. Cassing, and C. Greiner, Phys. Rev. D **69**, 025006 (2004).
[49] K. Zapp, J. Stachel, and U. A. Wiedemann, Phys. Rev. Lett. **103**, 152302 (2009).
[50] C. E. Coleman-Smith and B. Müller, Phys. Rev. C **86**, 054901 (2012).
[51] F. Senzel, O. Fochler, J. Uphoff, Z. Xu, and C. Greiner, arXiv:1309.1657.
[52] J. Uphoff, F. Senzel, Z. Xu, and C. Greiner, Phys. Rev. C **89**, 064906 (2014).
[53] R. Abir, C. Greiner, M. Martinez, M. G. Mustafa, and J. Uphoff, Phys. Rev. D **85**, 054012 (2012).